

12. Harrison, D. E. Vertical velocity in the central tropical Pacific—a circulation model perspective for JGOFS. *Deep-Sea Res. II* **43**(4–6), 687–705 (1996).
13. Toggweiler, J. R. & Carson, S. in *Upwelling the Ocean: Modern Processes and Ancient Records* (eds Summerhayes, C. et al.) 337–360 (Wiley, Chichester, 1995).
14. Wanninkhof, R. Relationship between wind speed and gas exchange over the ocean. *J. Geophys. Res.* **97**, 7373–7382 (1992).
15. Inoue, H. Y., Ishii, M., Matsueda, H. & Ahojima, M. Changes in longitudinal distributions of partial pressure of CO₂ (pCO₂) in the central and western equatorial Pacific, west of 160°W. *Geophys. Res. Lett.* **23**(14), 1781–1784 (1996).
16. Francey, R. J. et al. Changes in oceanic and terrestrial carbon uptake since 1982. *Nature* **373**, 326–330 (1995).
17. Ciais, P. et al. Partitioning of ocean and land uptake of CO₂ as inferred by CO₂ measurements from the NOAA/CMDL global air sampling network. *J. Geophys. Res.* **100**, 5051–5070 (1995).
18. Keeling, C. D., Whorf, T. P., Wahlen, M. & Vander Plicht, J. Interannual extremes in the rate of rise of atmospheric carbon dioxide since 1980. *Nature* **375**, 666–670 (1995).
19. Ciais, P., Tans, P. P., Trolier, M., White, J. W. & Francey, R. J. A large northern hemisphere terrestrial CO₂ sink indicated by the ¹³C/¹²C ratio of atmospheric CO₂. *Science* **269**, 1098–1102 (1995).
20. Maier-Reimer, E. & Hasselmann, K. Transport and storage of CO₂ in the ocean—An inorganic ocean-circulation carbon cycle model. *Clim. Dyn.* **2**, 63–90 (1987).
21. Tsuchiya, M., Lukas, R., Fine, R. A., Firing, E. & Lindstrom, E. Source waters of the Pacific Equatorial Undercurrent. *Prog. Oceanogr.* **23**, 101–147 (1990).
22. Toggweiler, J. R., Dixon, K. & Broecker, W. S. The Peru upwelling and the ventilation of the South Pacific thermocline. *J. Geophys. Res.* **96**, 20467–20497 (1991).
23. Quay, P. D. & Stuiver, M. Broecker upwelling rates for the equatorial Pacific Ocean derived from bomb ¹⁴C distribution. *J. Mar. Res.* **41**, 769–792 (1983).
24. Gu, D. & Philander, S. G. H. Interdecadal climate fluctuations that depend on exchanges between the tropics and extratropics. *Science* **275**, 805–807 (1997).
25. Murphy, P. P., Kelly, K. C., Feely, R. A. & Gammon, R. H. *Carbon Dioxide Concentrations in Surface Water and the Atmosphere: PMEL Cruises 1986–1989* (Tech. Memo. ERL PMEL-101 (DE95-009659), NOAA, Seattle, 1994).
26. Feely, R. A., Wanninkhof, R., Goyet, C., Archer, D. E. & Takahashi, T. Variability of CO₂ distributions and sea–air fluxes in the central and eastern equatorial Pacific during the 1991–94 El Niño. *Deep-Sea Res. II* **44**, 1851–1867 (1997).
27. Inoue, H. Y. et al. Long-term trend of the partial pressure of carbon dioxide (pCO₂) in surface waters of the western North Pacific, 1984–1993. *Tellus B* **47**, 391–413 (1995).
28. Winn, C. D., Li, Y.-H., Mackenzie, F. T. & Karl, D. M. Rising surface dissolved inorganic carbon at the Hawaii Ocean Time-series site. *Mar. Chem.* **60**(1–2), 33–48 (1998).
29. Wanninkhof, R. & Thoning, K. Measurement of CO₂ in surface water using continuous and discrete sampling methods. *Mar. Chem.* **44**, 189–205 (1993).
30. Keeling, C. D., Rakestraw, N. W. & Waterman, L. S. Carbon dioxide in the surface waters of the Pacific Ocean, 1—Measurements of the distribution. *J. Geophys. Res.* **70**, 6087–6097 (1965).

Acknowledgements. The assistance of the officers and crew of NOAA ships *Discoverer*, *Malcolm Baldrig*, and *Ka'imimoana* is acknowledged. We thank D.E. Harrison for wind data, and C. Cosca, M. Steckley and D. Ho for the pCO₂ measurements and data reduction. We also thank the NOAA TAO Project Office (director M. McPhaden) for support. This work was supported by the NOAA Climate and Global Change Program as part of the Ocean–Atmosphere Carbon Exchange Study.

Correspondence and requests for materials should be addressed to R.A.F. (e-mail: feely@pmel.noaa.gov).

Tectonic processes in Papua New Guinea and past productivity in the eastern equatorial Pacific Ocean

Mark. L. Wells*‡, Geoffrey K. Vallis† & Eli A. Silver‡

* School of Marine Sciences, University of Maine, Orono, Maine 04469, USA

‡ Institute of Marine Sciences, University of California, Santa Cruz, California 95064, USA

† GFDL, Princeton University, Princeton, New Jersey 08544, USA

Phytoplankton growth in the eastern equatorial Pacific Ocean today accounts for about half of the ‘new’ production—the fraction of primary production fuelled by externally supplied nutrients—in the global ocean. The recent demonstration that an inadequate supply of iron limits primary production in this region¹ supports earlier speculation that, in the past, fluctuations in the atmospheric deposition of iron-bearing dust may have driven large changes in productivity². But we argue here that only small (~2 nM) increases in the iron concentration in source waters of the upwelling Equatorial Undercurrent are needed to fuel intense diatom production across the entire eastern equatorial Pacific Ocean. Episodic increases in iron concentrations of this magnitude or larger were probably frequent in the past because a large component of the undercurrent originates in the convergent island-arc region of Papua New Guinea, which has experienced intensive volcanic, erosional and seismic activity over the past 16

million years. Cycles of plankton productivity recorded in eastern equatorial Pacific sediments may therefore reflect the influence of tectonic processes in the Papua New Guinea region superimposed on the effects of global climate forcing.

High-resolution sediment records in the eastern equatorial Pacific show strong cycling in silica:carbonate ratios resulting largely from the variable accumulation of diatom (silica) and coccolithophore (carbonate) tests³. These alternating conditions today reflect regimes having higher and lower productivity, respectively. Superimposed on these cycles are repeated episodes of extremely intense diatom production, manifested as laminated diatom deposits⁴. Increased upwelling of macronutrients driven by intensified global winds was thought to have been responsible for higher-productivity periods³, but a recent mesoscale enrichment study (IronEx II) showed¹ that diatom growth is limited by iron rather than inadequate supplies of nitrogen, phosphorus or silicon. The questions are now what magnitude of Fe inputs are needed to generate diatom bloom events and what was the frequency of these excursions?

Gauging the Fe perturbations required to stimulate diatom production reduces to two issues: (1) what is the lowest Fe concentration whereby uptake still permits maximum cellular growth rates, and (2) what Fe flux to surface waters is then needed to sustain high diatom productivity once this concentration threshold is surpassed? The distinction between concentration and flux is important, because it constrains the magnitude of events needed to generate intense diatom blooms. For example, maintaining relatively high (≥1 nM) Fe concentrations would require massive and persistent dust deposition because Fe is rapidly lost from surface waters⁵. In this case, significant global climate change must precede changes in diatom production. Conversely, if only low Fe concentrations are needed then flux requirements are substantially smaller, so that large shifts in productivity might

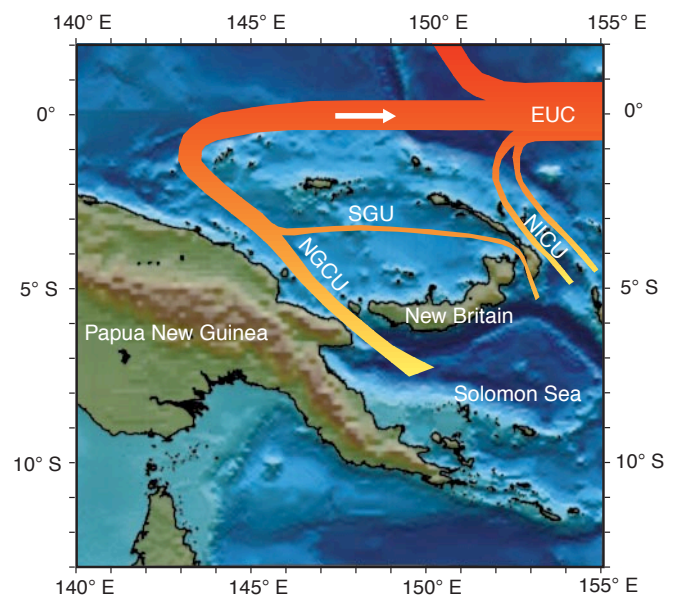


Figure 1 Source waters of the Equatorial Undercurrent (EUC). The New Guinea Coastal Undercurrent (NGCU) transports water at 200 m depth from the Solomon Sea, through the narrow Vitiaz Strait, and along the northern shelf margin of Papua New Guinea where it is joined by the St Georges Undercurrent (SGU)^{10,11}. The combined undercurrent turns north and then eastwards as the equatorial undercurrent. Additional undercurrents flowing north of New Ireland (the New Ireland Coastal Undercurrents, NICU), join the EUC, increasing its total flow. Subsurface waters north of the Equator also contribute to undercurrent flow; present estimates of the magnitude of this entrainment vary from small to roughly equal that of the southern inflows^{10,11}. Surface currents have been omitted for clarity.

Table 1 Iron upwelling fluxes needed to support diatom growth

Cellular Fe:carbon* ($\mu\text{mol Fe}:\text{mol C}$)	Fe upwelling flux† ($\text{nmol Fe m}^{-2}\text{d}^{-1}$)	Initial dissolved Fe‡ (nM)
2.4	360 (720)	2.1 (4.2)
4.0	600 (1,200)	3.4 (6.8)
6.0	900 (1,800)	5.2 (10.4)

* The range of cellular Fe quotas for oceanic phytoplankton determined in laboratory experiments⁷ and natural population cultures from equatorial Pacific surface waters¹⁵.

† Fe fluxes needed to support a calculated upwelling-nitrate-sustained new production rate of $150\text{ mmol C m}^{-2}\text{d}^{-1}$ at 90°W (off the Galapagos) as a function of diatom Fe quotas. The prerequisite Fe flux would decrease westwards along the Equator due to lower nitrate upwelling fluxes. Values in parenthesis are for maximum, non-sustainable bloom production ($300\text{ mmol C m}^{-2}\text{d}^{-1}$), such as occurred during IronEx II (that is, where nitrate concentration is drawn quickly to zero).

‡ The dissolved Fe concentrations in the PNG coastal undercurrent needed to support the required Fe upwelling flux at 90°W (near the eastern margin of the equatorial high-nitrogen, low-chlorophyll region).

possibly precede or occur independently of global climate change.

The threshold concentration where Fe uptake becomes diffusion-limited has been explored in models⁶ and contrived, well-defined laboratory culture experiments⁷. But predicting diffusion-limited conditions in ocean waters is difficult because we do not know which soluble chemical Fe species are directly accessed by phytoplankton⁸. Nonetheless, ambient soluble Fe concentrations (of species with molecular mass $<1\text{ kDa}$) only doubled to 40 pM Fe during IronEx II despite nanomolar Fe additions; the bulk of added Fe was sequestered into colloidal forms not directly accessible to the cell (M.L.W., manuscript in preparation). Thus it appears that massive dust deposition is not a prerequisite for dramatically altering productivity in the eastern equatorial Pacific.

The bulk of Fe input to equatorial surface waters occurs by advective upwelling from the Equatorial Undercurrent (EUC) rather than atmospheric deposition⁹. The possibility that undercurrent Fe inputs have varied during the past has not been explored. The EUC originates near Papua New Guinea (PNG) as a coalescence of at least four undercurrents, important components of which are the New Guinea Coastal Undercurrent (NGCU) and the St Georges Undercurrent (SGU) (Fig. 1). Both draw water from the Solomon Sea along the north coast of PNG before turning towards the Equator at $\sim 145^\circ\text{E}$ ^{10,11}. This core undercurrent is then joined by the New Ireland Coastal Undercurrents (NICU in Fig. 1) plus subsurface contributions from northern waters to form the EUC. The $\sim 500\text{-km}$ -wide, 100-m -thick EUC then travels $\sim 13,000\text{ km}$ constrained between 2°N and 2°S at speeds of $0.6\text{--}1.7\text{ m s}^{-1}$. It begins its equatorial transit at $\sim 200\text{ m}$ depth, but shoals gently upwards to surface south of the Galapagos Islands in the east. The New Guinea Coastal Undercurrent, the St Georges Undercurrent and the New Ireland Undercurrents are likely to strongly influence the dissolved Fe content of the EUC due to their very close proximity to land.

The loss of dissolved Fe from the ribbon-like EUC will largely result from advective upwelling into wind-mixed surface waters; turbulent diffusional losses will be small even with large ($\sim 10\text{ cm}^2\text{ s}^{-1}$) values of the vertical turbulent diffusivity coefficient. Using first-order approximations to model this loss (see Methods) suggests that Fe concentration in the upper EUC will fall exponentially during its passage across the Pacific Ocean. Lateral entrainment of water into the undercurrent¹² will probably further dilute the Fe concentration, perhaps by an additional factor of two. Scavenging losses to sinking particles will be small in relation to advective upwelling, given the comparatively low particle flux and high undercurrent speeds.

How well does this approach work? In this simplified model, Fe concentrations in the lower portion of the EUC will change little from those in the source waters while values in the upper segment decrease eastwards. Choosing a concentration of 0.35 nM Fe at 145°E yields a predicted value of $\sim 0.1\text{ nM Fe}$ in the upper portion of the EUC at 140°W , roughly halfway across the Pacific. These two values are nearly identical to those measured in the upper and lower portions of the EUC in this region⁹. Although no Fe data have been

reported for the New Guinea Coastal Undercurrent, the St Georges Undercurrent or the New Ireland Coastal Undercurrents, the 0.35 nM Fe value is remarkably close to that calculated (0.34 nM Fe) from reported oxygen values¹⁰ and a general $\text{O}_2:\text{Fe}$ relationship in the oceans¹³. Even with dilution of the EUC by entrainment during passage across the Pacific, this simplistic model provides a reasonable first approximation for calculating Fe upwelling fluxes across the eastern equatorial Pacific as a function of Fe concentrations in the coastal undercurrent.

We can judge the sensitivity of equatorial production to changes in dissolved Fe concentrations in EUC source waters by comparing model estimates of Fe upwelling fluxes with the Fe requirements for diatom growth. At 140°W , the upwelling flux of nitrate corresponds to a potential nitrate-sustained carbon production rate of $103\text{ mmol C m}^{-2}\text{d}^{-1}$ (ref. 9). A gradual 50% increase eastwards in the fugacity of CO_2 in surface water¹⁴ leads to corresponding nitrate-sustained production rates of $\sim 150\text{ mmol C m}^{-2}\text{d}^{-1}$ on the eastern margin of the equatorial Pacific. Seasonal variations in these estimates during a normal year will be comparatively small.

The calculated Fe flux needed to ensure that the upwelling nitrate fuels rapid diatom growth depends upon their cellular Fe quotas. Using the range of $2.4\text{--}6.2\text{ }\mu\text{mol Fe}:\text{mol C}$ measured in laboratory cultures⁷ and natural populations¹⁵ of oceanic diatoms, upwelling Fe fluxes of $360\text{--}900\text{ nmol m}^{-2}\text{d}^{-1}$ would be required to fully nourish diatom production (Table 1). The onset of rapid growth would occur 2–5 days after these increases in Fe upwelling flux (assuming a 50 m mixed depth and a 40 pM Fe threshold for optimal growth). According to our model, these Fe upwelling fluxes would require only 2–5 nM Fe in the coastal undercurrent feeding the EUC (Table 1, Fig. 2). Extremely intense diatom production, such as occurred during IronEx II ($\sim 300\text{ mmol C m}^{-2}\text{d}^{-1}$), would require 4–10 nM Fe in the source waters. Although these values are significantly higher than our present estimates for Fe in PNG undercurrents, they are similar to those measured in subsurface waters off the California shelf¹⁶. We now consider whether it is reasonable to expect such increases to have occurred in the past.

Papua New Guinea straddles a complex island arc junction of several plates¹⁷. During the Neogene period (23–1.6 Myr ago) there was significant crustal shortening and uplift in the New Guinea mobile belt, with extensive igneous activity occurring in the New Guinea Highlands during the middle Miocene epoch and again in the Pliocene epoch¹⁸. Between 16 to 3 Myr ago an extensive turbidite unit (called the Sukurum Formation), composed of volcanic and volcanoclastic rocks, was deposited along the northern margin of PNG, derived mainly from the Highlands region (Fig. 3)¹⁹. The Highlands uplift intensified dramatically during the late Miocene

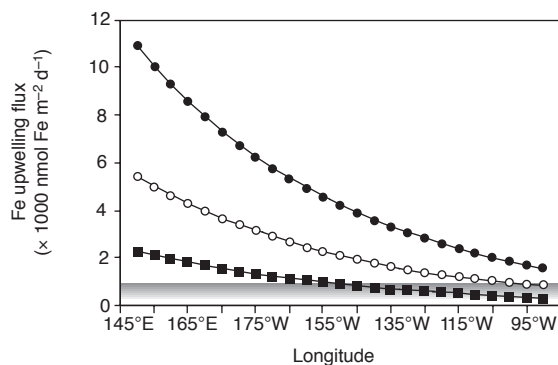


Figure 2 Estimated upwelling fluxes of iron. Iron fluxes from the EUC to surface waters vary as a function of longitude along the Equator and different starting Fe concentrations in the coastal undercurrents of PNG (filled squares, 2.1 nM Fe ; open circles, 5.0 nM Fe ; filled circles, 10.0 nM Fe). Shaded region indicates the range of upwelling Fe flux needed to support or surpass nitrate-sustained diatom blooms across the eastern equatorial Pacific (Table 1).

and early Pliocene (3–8 Myr ago)²⁰, along with uplift of the north-west margin of PNG resulting from the oblique collision with the New Guinea Highlands²¹. At approximately the time of this collision, the Manus basin began opening, the New Britain arc reversed itself, and the crust under Solomon Sea began subducting beneath the south margin of New Britain²².

Deep waters existed along the northern margin of PNG during this tectonic rearrangement²³, so it is reasonable to expect that the EUC source existed as a single shallow undercurrent constrained against the evolving PNG shelf by coriolis force, much as the New Guinea Coastal Undercurrent is today. Thus the undercurrent would have laid directly over the accumulating Sukurum Formation. The dramatic increase in erosion during the late Miocene to Pliocene (3–8 Myr ago) probably influenced undercurrent Fe concentrations through the partial dissolution of sinking particulates carried offshore in estuarine plumes as well as by turbidity currents induced by slumping of rapidly accumulating shelf sediments.

But by the middle Pliocene (3 Myr ago), uplift and erosion of the Highlands had abruptly decreased²⁴. The oblique collision and uplift of the Adelbert-Finisterre terrane above sea level during this interval also would have redirected the bulk of erosional debris towards the resultant embayment¹⁹, and displaced the undercurrent northwards away from the region of most intense sediment dispersal (Fig. 3).

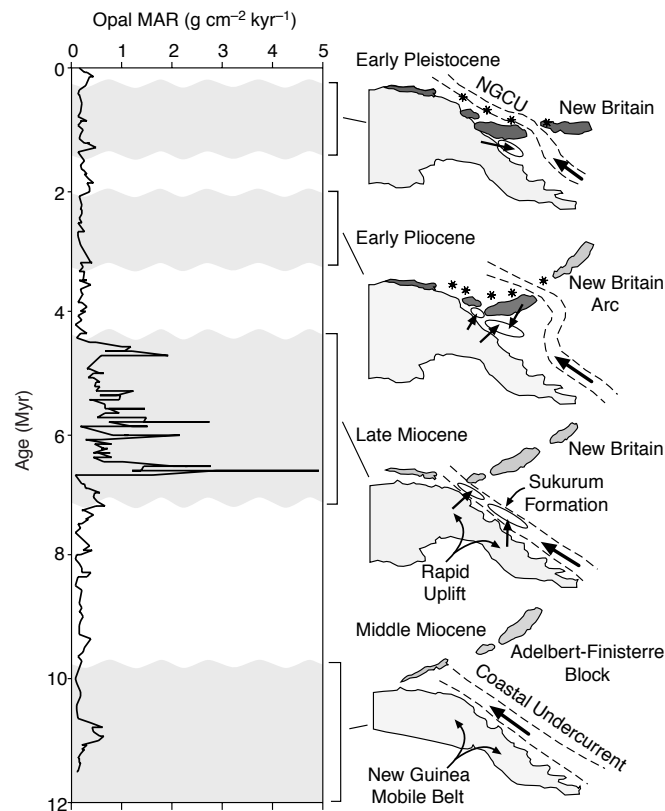


Figure 3 PNG tectonic sequence and eastern equatorial Pacific opal accumulation. Schematic representation of the PNG reconstruction is adapted from Abbott²¹. Right, the submarine (>500 m) Adelbert-Finisterre terrane is shown in light grey while the sub-aerial stages are in dark grey. The palaeo coastal undercurrent feeding the EUC is constrained along the shelf by Coriolis force. Arrows depict the undercurrent direction and the accumulation site of the Sukurum Formation. Asterisks indicate the position of the Bismarck arc comprising numerous volcanic centres. The approximate time line for collision and uplift of the Adelbert-Finisterre terrane is shown. Details of the location and orientation of the submarine terranes are less relevant than the timing of their uplift. Left, the opal mass accumulation rate (MAR) at the eastern equatorial site 849 of the Ocean Drilling Program Leg 138 corresponding to this time interval is shown for comparison³⁰.

During the late Pliocene epoch and the Quaternary period, continued uplift of New Britain, New Ireland and associated island chains of the Manus arc gradually fragmented the palaeo-undercurrent into the present assemblage of undercurrents.

This tectonic reconstruction²¹ suggests that Fe infusion of the EUC has fluctuated over the past 16 Myr, with inputs being most intense during the rapid uplift of the Highlands between ~3 and 8 Myr ago. This time interval corresponds to a period of extremely high opal accumulation in the eastern equatorial Pacific (Fig. 3). Although a paucity of geological data precludes a detailed reconstruction of PNG coastal geometry, the Adelbert-Finisterre terrane uplift was coeval with decreased diatom production (Fig. 3), suggesting a link between tectonics of PNG and high opal accumulation in the eastern equatorial Pacific. The same erosional process would have also infused the undercurrent with other bioactive metals and Si (ref. 25), ensuring that diatoms could flourish in eastern equatorial Pacific surface waters.

Aolian deposition in the eastern equatorial Pacific would have provided an additional source of Fe, and sediment records indeed show higher deposition occurred between 4 and 7 Myr ago. But these dust fluxes appear to have been only double present inputs²⁶, enough to perhaps stimulate diatom production but not enough to generate massive diatom blooms (Table 1). Moreover, aolian deposition seems unlikely to explain laminated diatom mats. These features signify very short periods of extremely high diatom production and extend >3,000 km along the Equator beneath the undercurrent⁴ ($\pm 2^\circ$ of the Equator) but not farther north where aolian fluxes were highest. The essential pulsed Fe inputs which fuelled these very large (>5 × 100 μm) diatoms have left no obvious terrigenous particulate signals.

We now consider the subtle control that erosional inputs may have exerted on the character of algal productivity. Comparatively large Fe enrichments (>~5 nM) of the coastal undercurrent could initiate massive diatom blooms across the entire eastern equatorial region (Table 1), where rapid N depletion would lead to sudden decreases ('crashes') in diatom populations, events that probably caused the formation of laminated diatom mats^{4,27}. These extensive mats appear sporadically between ~4 and 12 Myr ago, which coincides roughly with the Sukurum deposition in PNG. On the other hand, pulses or prolonged periods of moderate Fe enrichment of the coastal undercurrent would stimulate diatom growth over that of their smaller coccolithophore cousins, which could help explain the sub-Milankovitch cycling of silica:carbonate ratios observed in equatorial sediments. Depending on the balance with macronutrient inputs, moderate enrichments also might yield an east to west gradient in diatom production. Conversely, small Fe inputs would stimulate only coccolithophores, because their greater efficiency of Fe use and their smaller size allows them to out-compete diatoms under Fe-stress conditions⁷. Such enrichments might help to explain periods of high carbonate accumulation in equatorial sediments.

Erosion in PNG would probably also have enriched the EUC with the non-bioactive elements Al, Ti, Ba, Th, Po and Pb, which are metals used to help reconstruct palaeoproductivity. It remains to be evaluated whether these chemical proxies may at times have been compromised in the eastern equatorial Pacific.

The potential effect that erosion in the New Guinea Highlands exerted on productivity in the eastern equatorial Pacific would have diminished over the past ~4 Myr, when island emergence north of PNG partitioned the coastal undercurrent feeding the EUC into several smaller undercurrents (Fig. 1). Thus much larger Fe inputs to the New Guinea Coastal Undercurrent should now be required to equal the effects on productivity in the past. Nonetheless, the Bismarck and New Ireland volcanic arcs consist of hundreds of geologically recent eruptive centres and hydrothermal vent regions²⁸, suggesting that tectonics in the PNG region continue to influence sediment records of the eastern equatorial Pacific.

We recognize that climate forcing has unquestionably affected productivity in the eastern equatorial Pacific, and that equatorial sediment records reflect these impacts. But we argue that some aspect of this cycling has been driven by localized tectonic processes in the PNG island-arc region. The challenge is now to determine which patterns are linked to which driving mechanisms. □

Methods

Model description. A first-order approximation of the Fe loss due to upwelling from the EUC during its passage across the Pacific was given by assuming the advective upwelling flux of Fe is ϕw , where ϕ is the dissolved Fe concentration and w the vertical velocity. For a given initial Fe concentration in EUC source waters, the gradient of ϕ is calculated using $\partial\phi/\partial t = -\partial(w\phi)/\partial z$ by supposing that w is uniform across the Pacific ($\sim 1.23 \text{ m d}^{-1}$)²⁹ and Fe concentration falls linearly to zero over a vertical distance δz of 100 m; that is, from the core of the undercurrent at 150 m, across the undercurrent interface, to 50 m in the surface layer⁹. The resulting exponential fall in EUC dissolved Fe concentrations during its passage across the Pacific is described by $\phi = \phi_0 \exp(-x/x_0)$, where x is distance eastwards, $x_0 = u\delta z/w$, and u is an assumed mean undercurrent velocity ($\sim 1 \text{ m s}^{-1}$). Both w and u can be expected to vary somewhat, but the values chosen probably overestimate Fe depletion rates in the western equatorial Pacific, where upwelling velocities should be lower and undercurrent velocities higher.

Received 16 November 1998; accepted 16 February 1999.

- Coale, K. H. *et al.* A massive phytoplankton bloom induced by an ecosystem-scale iron fertilization experiment in the equatorial Pacific. *Nature* **383**, 495–501 (1996).
- Martin, J. H. Glacial–interglacial CO₂ change: the iron hypothesis. *Paleoceanography* **5**, 1–13 (1990).
- Pisias, N. G., Mayer, L. A. & Mix, A. C. Paleoceanography of the eastern equatorial Pacific during the Neogene: synthesis of Leg 138 drilling results. *Proc. ODP Sci. Res.* **138**, 5–24 (1995).
- Kemp, A. E. S. & Baldauf, J. G. Vast Neogene laminated diatom mat deposits from the eastern equatorial Pacific Ocean. *Nature* **362**, 141–144 (1993).
- Martin, J. H. *et al.* Testing the iron hypothesis in ecosystems of the equatorial Pacific Ocean. *Nature* **371**, 123–129 (1994).
- Hudson, R. J. M. & Morel, F. M. M. Iron transport in marine phytoplankton: Kinetics of cellular and medium coordination reactions. *Limnol. Oceanogr.* **35**, 1002–1020 (1990).
- Sunda, W. G. & Huntsman, S. A. Iron uptake and growth limitation in oceanic and coastal phytoplankton. *Mar. Chem.* **50**, 189–206 (1995).
- Wells, M. L., Price, N. M. & Bruland, K. W. Iron chemistry in seawater and its relationship to phytoplankton: a progress report. *Mar. Chem.* **48**, 157–182 (1995).
- Coale, K. H., Fitzwater, S. E., Gordon, R. M., Johnson, K. S. & Barber, R. T. Control of community growth and export production by upwelled iron in the equatorial Pacific Ocean. *Nature* **379**, 621–624 (1996).
- Tsuchiya, M., Lukas, R., Fine, R. A., Firing, E. & Lindstrom, E. Source waters of the Pacific equatorial undercurrent. *Prog. Oceanogr.* **23**, 101–147 (1989).
- Butt, J. & Lindstrom, E. Currents off the east coast of New Ireland, Papua New Guinea, and the relevance to regional undercurrents in the western Equatorial Pacific Ocean. *J. Geophys. Res.* **99**, 12503–12514 (1994).
- Philander, S. G. H., Hurlin, W. J. & Seigel, A. D. Simulation of the seasonal cycle of the tropical Pacific Ocean. *J. Phys. Oceanogr.* **17**, 1986–2002 (1987).
- Martin, J. H., Gordon, R. M., Fitzwater, S. & Broenkow, W. W. Vertex: phytoplankton/iron studies in the Gulf of Alaska. *Deep Sea Res.* **36**, 649–680 (1989).
- Murray, J. W., Barber, R. T., Roman, R. R., Bacon, M. P. & Feely, R. A. Physical and biological controls on carbon cycling in the equatorial Pacific. *Science* **266**, 58–65 (1994).
- Takeda, S. & Obata, H. Response of equatorial Pacific phytoplankton to submillimolar Fe enrichment. *Mar. Chem.* **50**, 219–227 (1995).
- Landing, W. M. & Bruland, K. W. The contrasting biogeochemistry of iron and manganese in the Pacific Ocean. *Geochim. Cosmochim. Acta* **51**, 29–43 (1987).
- Tregoning, P. *et al.* Estimation of current plate motions in Papua New Guinea from Global Positioning System observations. *J. Geophys. Res.* **103**, 12181–12203 (1998).
- Rogerson, R. J. *et al.* *The Geology and Mineral Resources of the Sepik Headwaters Region, Papua New Guinea* (Geological Survey of Papua New Guinea, Port Moresby, 1987).
- Abbott, L. D. *et al.* Stratigraphic constraints on the development and timing of arc–continent collision in northern Papua–New Guinea. *J. Sedim. Res. B* **64**, 169–183 (1994).
- Hill, K. C. & Gleadow, A. J. W. Uplift and thermal history of the Papuan fold belt, Papua New Guinea: apatite fission track analysis. *Austr. J. Earth Sci.* **36**, 515–539 (1989).
- Abbott, L. D. Neogene tectonic reconstruction of the Adelbert–Finisterre New Britain collision, northern Papua New Guinea. *J. S. Asian Earth Sci.* **11**, 33–51 (1995).
- Musgrave, R. J. Paleomagnetism and tectonics of Malaita, Solomon Islands. *Tectonics* **9**, 735–759 (1990).
- Abbott, L. D. *et al.* Measurement of tectonic surface uplift rate in a young collisional mountain belt. *Nature* **385**, 501–507 (1997).
- Crowhurst, P. V., Hill, K. C. & Foster, D. A. in *Proc. PNG Geology, Exploration and Mining Conf.* (ed. Hancock, G. E.) 51–60 (Australian Inst. of Mining and Metallurgy, Melbourne, 1997).
- Dugdale, R. C. & Wilkerson, F. P. Silicate regulation of new production in the equatorial Pacific upwelling. *Nature* **391**, 270–273 (1998).
- Hovan, S. A. Late Cenozoic atmospheric circulation intensity and climatic history recorded by eolian deposition in the eastern equatorial Pacific Ocean, Leg 138. *Proc. ODP Sci. Res.* **138**, 615–625 (1995).
- Kemp, A. E. S., Baldauf, J. G. & Pearce, R. B. Origins and paleoceanographic significance of laminated diatom ooze from the eastern equatorial Pacific Ocean. *Proc. ODP Sci. Res.* **138**, 641–646 (1995).
- Auzende, J.-M. *et al.* Activité tectonique, magmatique et hydrothermale dans le bassin de Manus (SW Pacifique, Papouasie-Nouvelle Guinée): campagne MANUSFLUX du Shinkai-6500. *CR Acad. Sci. Paris* **323**, 501–508 (1996).

- Bryden, H. L. & Brady, E. C. Diagnostic model of the three-dimensional circulation in the upper equatorial Pacific Ocean. *J. Phys. Oceanogr.* **15**, 1255–1273 (1985).
- Farrell, J. W. *et al.* Late Neogene sedimentation patterns in the eastern equatorial Pacific Ocean. *Proc. ODP Sci. Res.* **138**, 717–753 (1995).

Acknowledgements. We thank L. D. Abbott, T. F. Pedersen and J. R. Toggweiler for comments. This work was supported by the NSF Chemical Oceanography Program.

Correspondence and requests for materials should be addressed to M.L.W. (e-mail: mlwells@maine.edu).

Partitioning of nickel and cobalt between silicate perovskite and metal at pressures up to 80 GPa

O. Tschauner*, A. Zerr*, S. Specht*, A. Rocholl†, R. Boehler* & H. Palme‡

* Max-Planck-Institut für Chemie, Postfach 3020, 55020 Mainz, Germany

† Mineralogisches Institut, Universität Heidelberg, Im Neuenheimer Feld 236, 69120 Heidelberg, Germany

‡ Institut für Mineralogie und Geochemie, Universität Köln, Zùlpicher Straße 49b, 50674 Köln, Germany

The high abundance of both nickel and cobalt and the chondritic Ni/Co ratio found in samples derived from the Earth's mantle are at odds with results from laboratory-based partitioning experiments conducted at pressures up to 27 GPa (refs 1,2). The laboratory results predict that the mantle should have a much lower abundance of both Ni and Co and a considerably lower Ni/Co ratio owing to the preferential partitioning of these elements into the iron core. Two models have been put forward to explain these discrepancies: homogeneous accretion^{3–6} (involving changes of the Ni and Co partition coefficients with oxygen and sulphur fugacities, pressure and temperature) and heterogeneous accretion^{7–9} (the addition of chondritic meteorites to the mantle after core formation was almost complete). Here we report diamond-cell experiments on the partitioning of Ni and Co between the main lower-mantle mineral ((Mg,Fe)SiO₃-perovskite) and an iron-rich metal alloy at pressures up to 80 GPa (corresponding to a depth of $\sim 1,900$ km). Our results show that both elements become much less siderophilic with increasing pressure, such that the abundance of both Ni and Co and the Ni/Co ratio observed in samples derived from the Earth's mantle appear to indeed be consistent with a homogeneous accretion model.

Heterogeneous accretion models have garnered much support as an explanation of the high abundance of Ni and Co in the Earth's upper mantle¹⁰. This support is based on studies on the partitioning of these elements between metal and silicate phases up to pressures of 27 GPa (refs 11–16) which did not show convergence to equal partitioning of Ni and Co as required in order to preserve their observed chondritic ratio. However, studies^{5,6} on liquid metal-silicate systems showed that this chondritic ratio may be preserved under certain conditions of pressure and temperature in an early, sulphur-rich magma ocean. None of these studies, however, addressed the partitioning behaviour of Ni and Co at lower-mantle conditions experimentally. About 80% of the lower mantle consists of (Mg,Fe)SiO₃-perovskite (hereafter called perovskite). Because of the high melting temperature of this phase at high pressure¹⁷, a substantial amount of solid perovskite was probably present in the early Earth during core formation. Models for the interaction between iron and perovskite are nearly unconstrained by experimental data: only few data exist on perovskite/metal partitioning of Ni and Co at pressures of the uppermost lower mantle^{11,12}. The chemical exchange of siderophile elements between perovskite and metal at very high pressure is also important for understanding